Proceedings of the ASME 2015 International Mechanical Engineering Congress and Exposition
IMECE2015
November 13-19, 2015, Houston, Texas

IMECE2015-50597

INNOVATIVE VOLUMETRIC SOLAR RECEIVER MICRO-DESIGN BASED ON NUMERICAL PREDICTIONS

Raffaele Capuano
German Aerospace Center (DLR)
Juelich, Germany

Thomas Fend
German Aerospace Center (DLR)
Cologne, Germany

Bernhard Hoffschmidt
German Aerospace Center (DLR)
Cologne, Germany

Robert Pitz-Paal
German Aerospace Center (DLR)
Cologne, Germany

ABSTRACT

Due to the continuous global increase in energy demand, Concentrated Solar Power (CSP) represents an excellent alternative, or add-on to existing systems for the production of energy on a large scale.
In some of these systems, the Solar Power Tower plants (SPT), the conversion of solar radiation into heat occurs in certain components defined as solar receivers, placed in correspondence of the focus of the reflected sunlight.
In a particular type of solar receivers, defined as volumetric, the use of porous materials is foreseen. These receivers are characterized by a porous structure called absorber. The latter, hit by the reflected solar radiation, transfers the heat to the evolving fluid, generally air subject to natural convection.

The proper design of these elements is essential in order to achieve high efficiencies, making such structures extremely beneficial for the overall performances of the energy production process.

In the following study, a parametric analysis and an optimized characterization of the structure have been performed with the use of self-developed numerical models.
The knowledge and results gained through this study have been used to define an optimization path in order to improve the absorber microstructure, starting from the current in-house *state-of-the-art* technology until obtaining a new advanced geometry.

NOMENCLATURE

Latin symbols

G	Irradiation source [$W \cdot m^{-2}$]
A_v	Specific surface area [$m^2 \cdot m^{-3}$]
T	Temperature [K]
P	Pressure [Pa]
k	Thermal conductivity [$W \cdot m^{-1} \cdot K^{-1}$]
c_p	Specific heat capacity [$J \cdot kg^{-1} \cdot K^{-1}$]
h	Heat transfer coefficient [$W \cdot m^{-2} \cdot K$]
$h \cdot A_v$	Volumetric heat transfer coefficient [$W \cdot m^{-3} \cdot K$]
$\dot{m}$	Fluid mass flow rate [$kg \cdot s^{-1}$]
J	Radiosity [$W \cdot m^{-2}$]

Greek symbols

ε	Porosity
α	Absorption coefficient [m^{-1}]
σ	Stefan-Boltzmann constant [$W \cdot m^{-2} \cdot K^{-4}$]
σ_s	Scattering coefficient [m^{-1}]
ρ	Density [$kg \cdot m^{-3}$]
μ	Dynamic viscosity [$kg\ m^{-1}\ s^{-1}$]
η	Efficiency
$\hat{\alpha}$	Material absorptivity

Subscripts

f	Fluid
s	Solid
h	Homogeneous volume

in	Inlet
out	Outlet
i.s.	Innovative structure
s-o-a	State-of-the-art
c	Ceramic
a	Metallic alloy
m	Mutual
ext	External
amb	Ambient

INTRODUCTION

The growing energy needs and environmental concern have led in recent years to the use of alternative sources of energy. One of the options is undoubtedly solar energy. However, since only a small fraction of the radiation produced by the sun reaches the Earth, optical concentration systems are needed in order to reach high flux values useful in industrial applications.

Among the systems used to make use of the solar energy source there is the Concentrated Solar Power (CSP). Those systems use mirrors or lenses to concentrate the solar radiation at a focal point or line. The focused light is then transformed into heat, which drives a thermal engine connected to an electric power generator.

One of the configurations that the CSP systems can assume is the Solar Power Tower (SPT) plant. Here, the sunlight is reflected from a vast array of mirrors (solar field) and focused at a single point placed at the upper end of the tower. In correspondence with the focal point, there is the solar receiver. In some of those plants, it is defined as open volumetric receiver since it is characterized by a porous solid (absorber) crossed by atmospheric air that will be heated by contact with the inner walls. Subsequently, the hot air is then used for industrial purposes, such as steam production in Rankine turbine-generator systems in place of fossil fuels [1].

Several types of volumetric absorbers have been built and tested, such as metallic wire mesh [2], ceramic fibers [3], packed bed particles [4], honeycombs [5] and foams [6].

This entire variety of different structures can be recognized and characterized by parameters and coefficients, defined as effective properties, like the porosity (ε), that is the ratio between the void volume and the total volume of the porous absorber, the absorption (α) and the scattering (σ_s) coefficients, that defines the attenuation of the radiation in such structures, the specific surface area (A_v) which is the index of the exchange surface in porous materials, defined as the ratio of the wet surface and the corresponding volume, and the convective heat transfer coefficient (h), defined as the ratio of the heat flux and the thermodynamic driving force, in this case the temperature difference between the atmospheric flow and the inner surfaces.

In order to achieve high efficiencies in the conversion of the incoming sunlight into usable heat, a good combination of those parameters is needed.

For this purpose, a numerical analysis, showing the effect of these properties on the overall performances of the receiver, using a simplified numerical approach, represents a useful preliminary work for the successive design procedure.

The same approach has been taken up by several research groups, as it turned out to be very convenient due to its computational convenience and ability to simulate very complex structures.

Petrasch et al. [7] used a homogeneous numerical approach for the characterization of the radiative heat transfer through a two-phase media. Caliot et al. [8] studied the heat exchange in reticulated porous ceramics to be used in solar thermal application through simplified homogeneous model.

In 2010, Smirnova et al. [9] compared the results of the heat transfer analysis in a volumetric air receiver using both homogeneous and inhomogeneous simulation approaches.

Furthermore, Kribus et al. [10] investigated the possible performance of volumetric absorbers as a function of geometric and material properties, aiming to identify an optimum combination.

On the other hand, a simplified approach is not the only way to study the performance of a volumetric solar absorber. Detailed models may also be applied, using as computational domain the elementary unit of the receiver that could be a single channel, a foam cell or a random unit, according to the structure geometry.

In the same work of Smirnova et al. [9], an inhomogeneous model is used for the evaluation of the performances of a volumetric solar receiver with a honeycomb-based geometry. Here, a 3D single channel represents the control volume used in the numerical calculation.

Wu et al. [11] used a tetrakaidecahedron model for the representation of the unit element of ceramic foam used as a volumetric solar receiver.

In the present study, a porous innovative structure has been designed in order to obtain high performance as volumetric solar receiver.

Prior to this work, a preliminary parametric study has been carried out to characterize the effects of the parameters that have most influence on the design of such structures, using a self-developed numerical model. It is defined as continuum simulation approach and is based on a simplified representation of the porous medium. Here, the porous absorber consists of a homogeneous volume characterized by the set of effective properties previously introduced.

The effect of the variation of these properties has been analysed in order to figure out the best combination in terms of design of such structures, taking into account current production limits.

The results obtained at the end of the sensitivity study have been used for the design of a brand new porous structure that has led to an improved heat exchange and a better efficiency.

The structure has been numerically tested with the use of a second self-developed CFD model, based on the detailed representation of the absorber unit element and compared to the in-house state-of-the-art.

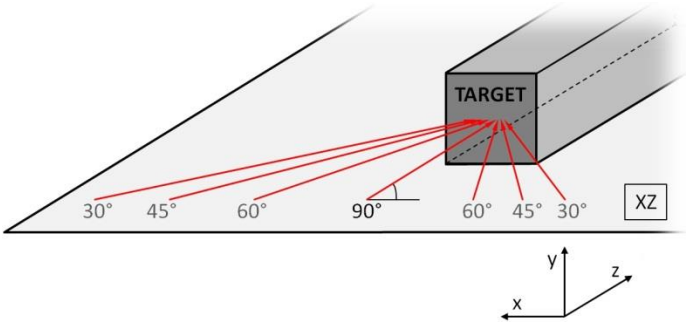

Figure 1a – Radiation incoming direction – plane XZ.

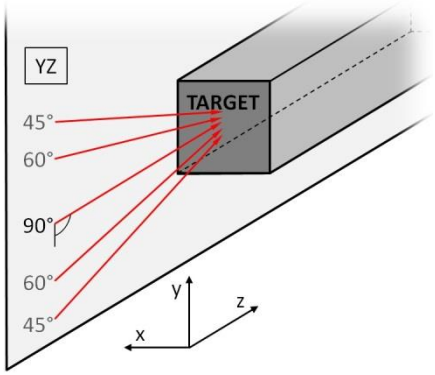

Figure 1b – Radiation incoming direction – plane YZ.

At last, the innovative geometry will be produced in the form of sample prototype by an in-house company for the subsequent experimental tests.

MATERIALS AND METHODS

The proposed study aims to design a new porous structure to be used as volumetric receiver in solar thermal power plants.
The methodology used consists of two separate phases.
The first phase involves the analysis of the variation of the effective properties on the performance of the absorber in solar thermal applications. Herein, a portion of the absorber is represented by a homogeneous volume and a set of effective properties, whose variation has been analyzed in order to identify the best combination for optimal performance. In this way, a *designing path* has been detected and applied for the subsequent actual design procedure.

As a result, an innovative structure has been drawn and it has been numerically tested in the second phase, with the use of a second detailed numerical model

For the purposes listed above, two different numerical models have been developed and used for the heat and mass transfer analysis in porous materials. They are both based on a three-dimensional representation of the porous volume and calculate the heat exchange between the solid phase and the fluid flowing into the porous zone under forced convection.
Those models can be defined as follow:

- continuum model,
- discrete model.

The first one evaluates the conjugate heat transfer inside a homogeneous volume characterizing the porous absorber by means of the effective properties. Thus, no detailed representation of the porous structure is needed, drastically reducing the simulation time and memory requirements [12]. For this simulation scenario, radiation in participating media has been considered, setting a diffuse irradiation condition as main energy source (G_h), due to software constraints. Thus, the Discrete Ordinates (DO) approximation method has been applied for the solution of the Radiative Transfer Equation (RTE) [13].

The discrete model is based on the accurate characterization of the absorber, represented by its unit element and analyzed with the use of symmetrical boundaries. Thus, a CFD simulation is set for the evaluation of the conjugate heat transfer. The main assumptions behind the mathematical model are steady-state, incompressible flow, homogeneous properties of the gaseous and solid phases, grey body solid surfaces. The gaseous and solid phases can be at different temperatures and the local thermal non-equilibrium equations (LTNE) are used.

The radiative heat transfer is treated by using the direct area integration method through view factor calculations. The radiative source has been set taking into account the setup of the HLS solar simulator and calibrated in respect of previously determined experimental conditions [14]. The incoming irradiation (G) has been distributed on different vectors at different incoming angles, ranging from 90° to 30° compared to the normal to the YZ and XZ planes, placed on XZ and YZ planes respectively, as shown in Fig. 1a and Fig. 1b.

Both models have been previously compared and validated with several numerical and experimental results, referring to the current in-house *state-of-the-art* geometry and other material samples [15].

Continuum model – physical and mathematical description

A homogeneous 3D volume, representing an arbitrary portion of the absorber made out of ceramic material, is used in the continuum model.

In this particular case, as shown in Fig. 2a, a parallelepiped represents the porous zone; it has a front square surface (A_1) of 1×10^{-4} m^2 and a depth of 5×10^{-2} m.
Concerning the fluid volume, an inlet zone, 3×10^{-3} m deep, is coupled to a solid of the same size as that one characterizing the porous volume, as shown in Figure 2b.
The fluid and the porous volumes, then, are overlapped on each other in order to simulate the air flow through porous medium under atmospheric conditions.

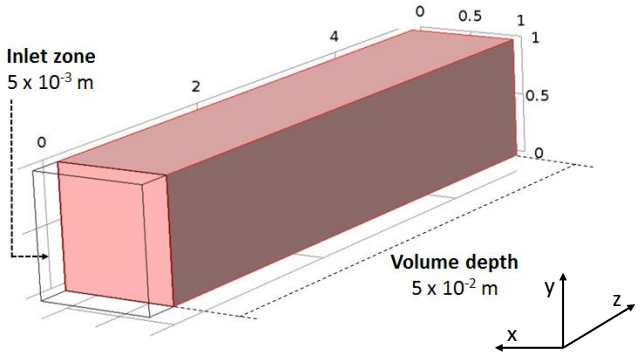

Figure 2a – Homogeneous volume.

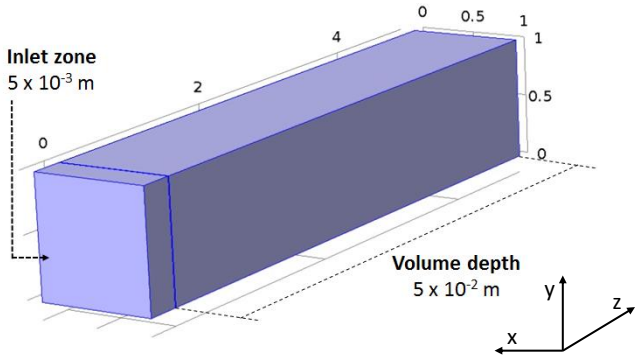

Figure 2b – Fluid volume.

For the characterization of the porous zone, weighted and effective properties have been used: properties referred to the homogeneous phase like the thermal conductivity (k_h), the density (ρ) and the specific heat capacity (c_p) have been weighted in relation to the porosity of the structure in order to take into account the presence of the air in the homogeneous volume and its corresponding properties. Other quantities like the volumetric heat transfer coefficient, defined as the product of the convective heat transfer coefficient and the specific surface area ($h \cdot A_v$), and optical parameters like the absorption and scattering coefficients can be obtained either experimentally, from literature or from detailed numerical simulation [16-19].

Numerical equations

For the numerical calculation of the velocity and pressure fields the Navier-Stokes equations have been used in the model. This application mode describes the connection of the fluid velocity and the pressure according to the equation:

$$\nabla\left(-p + \mu(\nabla u + (\nabla u)^T)\right) = \rho(u\nabla)\, u \qquad (1)$$

where μ is the dynamic viscosity, u is the fluid velocity and ρ is the fluid density and:

$$\nabla(\rho u) = 0;\ \rho = \rho(p, T_f) \qquad (2)$$

The heat transfer in the air has been simulated according to the following equation:

$$\nabla\left(-k_f \nabla T_f + \rho c_p u T_f\right) = Q_{f\to h} \qquad (3)$$

where k_f is the fluid thermal conductivity and c_p is the fluid heat capacity. The heating power from the fluid to the homogeneous volume $Q_{f\to h}$ has been determined through the volumetric heat transfer coefficient ($h \cdot A_v$) according to the following equation:

$$Q_{f\to h} = Q_{h\to f} = hA_v(T_h - T_f) \qquad (4)$$

where T_h is the temperature of the homogeneous phase. The heat transfer in the latter has been simulated through the heat conduction module, based on the Fourier equation:

$$-\nabla(k_h \nabla T_h) = Q_{h\to f} + Q_r \qquad (5)$$

where $Q_{h\to f}$ is the heating power from the homogeneous volume to the fluid phase and k_h is the thermal conductivity of the porous volume. Qr represents the power related to the radiative source term and it can be defined as follow:

$$Q_r = \alpha(G_h - \sigma T_h^4) \qquad (6)$$

where α is the absorption coefficient and σ is the Stefan-Boltzmann constant.
The radiative source has been evaluated through the Radiative Thermal Equation, adapted to the Discrete Ordinates solution method and can be expressed as follow:

$$\bar{s} \cdot I(\bar{s}) = \alpha I_b(T_h) - (\alpha + \sigma_s) I(\bar{s}) + \frac{\sigma_s}{4\pi}\int_0^{4\pi} I(\bar{s}')\varphi(\bar{s}', \bar{s})\, d\bar{s}' \qquad (7)$$

where $I(\bar{s})$ is the radiative intensity in the $\bar{s}$ direction, φ is the scattering phase function and I_b is the blackbody radiative intensity which is expressed as follow:

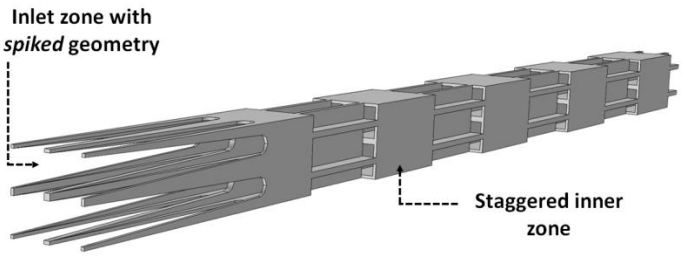

Figure 3a – Perspective view of the innovative geometry unit element.

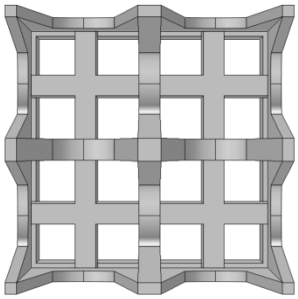

Figure 3b – Front view of the innovative geometry unit element.

$$I_b(T_h) = \frac{n^2 \sigma T^4}{\pi} \quad (8)$$

where n is the refractive index of the participating media. Furthermore, in this set of simulations the scattering has been considered isotropic, thus the phase function $\varphi(\bar{s}', \bar{s})$ is equal to 1.

Discrete model – physical and mathematical description

An innovative honeycomb-base porous structure, which unit element is shown in Fig. 3a and Fig. 3b, has been designed following the indications obtained with the use of the previously introduced parametric study through continuum simulation and is currently under patenting process.

The structure, representing the solid volume in the numerical discrete simulation, presents a graded porosity. It is characterized by an entrance area with a particular spike-profile, in correspondence of which, the value of the porosity passes from 0.98 to 0.70 of the rear zone.
The thickness of the inner walls is 200 microns, thus obtaining a high cellularity and therefore a high volumetric heat transfer coefficient.

In addition, a staggered geometry characterizes the inner structure. In this way, the turbulence of the atmospheric air flow increases, thereby increasing the volumetric heat transfer coefficient.

The fluid volume is reported in Fig. 4. Also in the detailed model, a fictitious inlet zone is present for the development of the flow.

Numerical equations

The numerical calculation of the velocity and pressure fields of the air flow is based, yet again, on the Navier-Stokes formulation, using Eq. 1 and Eq. 2 as Momentum and Continuity equations respectively.

The energy exchange has been treated using the Fourier´s law for the solid and fluid phases through the following equations:

Fluid phase

$$\rho c_p u \nabla T_f = \nabla(k_f \nabla T_f) \quad (9)$$

Solid phase

$$-\nabla(k_s \nabla T_s) = Q_r \quad (10)$$

$$Q_r = \alpha(G - \sigma T_s^4) \quad (11)$$

$$G = G_m(J) + F_{amb}\, \sigma T_{amb}^4 + G_{ext} \quad (12)$$

where G_m is the mutual irradiation, coming from other boundaries in the model, J is the radiosity, which is the sum of the reflected and emitted radiation that leaves the surface.
G_{ext} is the irradiation from external radiation sources, defined as the sum of the products, for each external source, of the external heat sources view factor by the corresponding source radiosity and F_{amb} is an ambient view factor whose value is equal to the fraction of the field of view that is not covered by other boundaries.

A more detailed description of the numerical approach, including boundary and continuity conditions, is presented in [20].

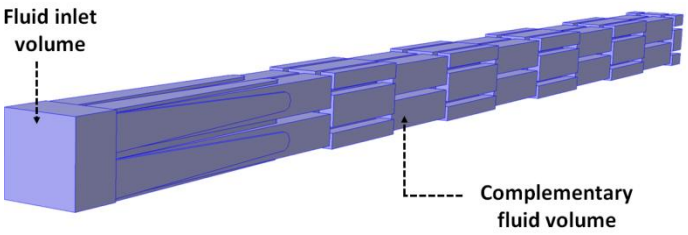

Figure 4 – Complementary fluid volume for the discrete model

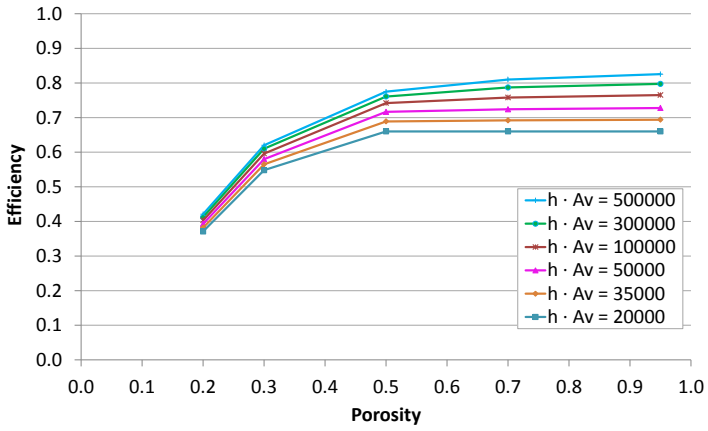

Figure 5 – Efficiency vs porosity for $(h \cdot A_v) = (2.0, 3.5, 5.0, 10.0, 30.0, 50.0) \times 10^4\ W \cdot m^{-3} \cdot K$.

RESULTS

In the following section, the results of the parametric study obtained through continuum simulation and the ones obtained through discrete simulation will be shown in two different sub-paragraphs.

Continuum model – parametric study results

A sensitivity study on the effect of the variation of the effective properties on the overall performances of the solar absorber has been performed with the use of the continuum model.
Here, several simulation processes have been conducted considering the same initial conditions such as a diffuse irradiation source, homogeneous thermal conductivity, fluid incoming mass flow rate ($\dot{m}$) and thermodynamic conditions defined as follow:

- $G_h = 6.5 \times 10^5\ W \cdot m^{-2}$;
- $\dot{m} = 4.3 \times 10^{-5}\ kg \cdot s^{-1}$;
- $k_h = (1-\varepsilon) \cdot k_{s\text{-}c}(T_s) + \varepsilon \cdot k_f\ W \cdot m^{-1} \cdot K^{-1}$;
- $T_{f-in} = 318.25\ K$;
- $P_{f-in} = P_{f-out} = 101325\ Pa$;

where k_f is the fluid thermal conductivity and $k_{s\text{-}c}(T_s)$ is the material thermal conductivity as a function of the solid temperature that ranges from 150 $W \cdot m^{-1} \cdot K^{-1}$ at room temperature to 40 $W \cdot m^{-1} \cdot K^{-1}$ at 800 °C [21].

This study has been carried out in two steps: in the first, defined as *Stage 1*, the effect of the variation of the porosity and the volumetric heat transfer coefficient has been analyzed, setting the values of the optical parameters as reported below:

- $\alpha = 115\ m^{-1}$;
- $\sigma = 13\ m^{-1}$.

Therefore, an array of values for the porosity and the volumetric heat transfer coefficient has been set as follows:

- $\varepsilon = 0.20, 0.30, 0.50, 0.70, 0.95$;
- $h \cdot A_v = (2.0, 3.5, 5.0, 10.0, 30.0, 50.0) \times 10^4\ W \cdot m^{-3} \cdot K$.

During the second step, defined *Stage 2*, also the optical parameters has been taken into account. Thus, an array of values for the following properties has been chosen:

- $\varepsilon = 0.50, 0.95$;
- $h \cdot A_v = (5.0, 10.0, 30.0, 50.0) \times 10^4\ W \cdot m^{-3} \cdot K$;
- $\alpha = (15, 35, 50, 100, 150)\ m^{-1}$;
- $\sigma = (10, 200)\ m^{-1}$.

The efficiency (η), defined as the ratio between the incoming radiative heat flux and the enthalpy gained by the fluid during the conjugate heat transfer, is considered as a comparison parameter.
It has been defined with the following equation:

$$\eta = \frac{\left(\dot{m} \cdot c_p \cdot (T_{f-out} - T_{f-in})\right)}{(I_d \cdot A_1)} \qquad (13)$$

Stage 1 results

The chart in Fig. 5 shows the variation of the efficiency versus the porosity for different volumetric heat transfer coefficients, given the value of the optical properties as previously reported in the paragraph.

The highest values of the efficiency correspond to structures presenting high porosity and high volumetric heat transfer coefficient. High values of porosity facilitate the penetration of the radiation inside the porous volume; therefore radiative energy is not stuck in the front zone, leading to a lower temperature of the solid and thus in lower radiative emission losses [10].
At the same time, a high volumetric heat transfer coefficient also ensures a better performance of the absorber. In order to obtain this condition, it is possible to operate both from a fluid-dynamic point of view, acting directly on the convective heat transfer coefficient, and at the structural level, using an absorber which present high exchange surface area and, therefore, high cellularity.

Stage 2 results

The charts in Fig. 6a and Fig. 6b show the trend of the efficiency versus the different absorption coefficients considered in this second group of simulations, for two values of porosity, different volumetric heat transfer coefficients (5, 10, 30, 50 x $10^4\ W \cdot m^{-3} \cdot K$) are considered and scattering equal to 10 and 200 m^{-1}.

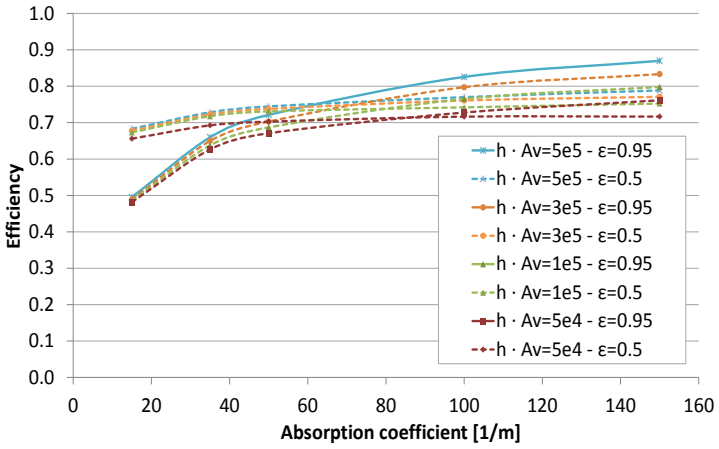

Figure 6a – Efficiency vs absorption for $(h \cdot A_v)$ = (5.0, 10.0, 30.0, 50.0) x 10^4 W · m^{-3} · K, ε = (0.50, 0.95) and σ = 10 m^{-1}.

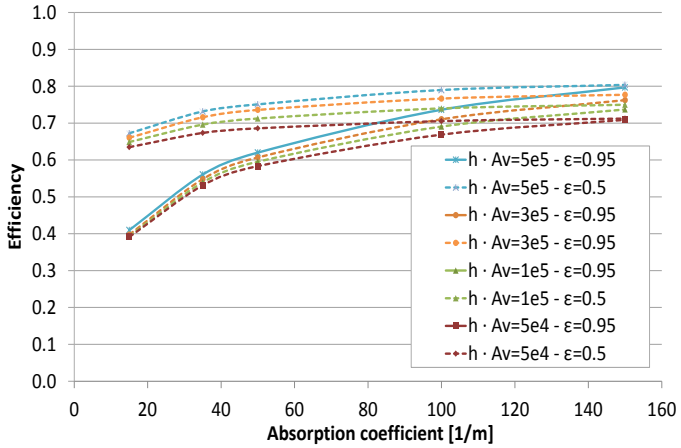

Figure 6b – Efficiency vs absorption for $(h \cdot A_v)$ = (5.0, 10.0, 30.0, 50.0) x 10^4 W · m^{-3} · K, ε = (0.50, 0.95) and σ = 200 m^{-1}.

The unfavorable effect of the scattering is more evident in high porosity structures; here the void volume is bigger and there is a higher possibility of losing part of the radiation as a consequence of the inner multiple reflections caused by high scattering values. On the other hand, a higher inner reflection in dense structures allows a higher gaining in term of radiative heat flux since the possibilities of leaving the volume are lower compared to high porosity geometries.

As shown in the charts reported above, higher performances are obtained in correspondence of structures with high absorption coefficient and high volumetric heat transfer coefficient. On the other hand, when the value of the absorption is low, part of the incoming radiation is lost, leaving the computational domain without taking part in the heat transfer process, as shown in Fig. 7. Here, the attenuation curve of the radiative source is reported in relation to the depth of the absorber, for the two extreme values of the absorption coefficient array and the two porosities, chosen the scattering and the volumetric heat transfer coefficients (σ = 10 m^{-1}, $(h \cdot A_v)$ = 3.0 x 10^4 W · m^{-3} · K). In both cases, in correspondence of the low absorption curves, an aliquot of the incoming radiation leaves the volume, lowering the overall performances. Furthermore, the low porosity curves also present a lower initial value of the entering radiation due to the higher percentage of solid in the homogeneous phase that reaches a higher temperature in correspondence of the inlet zone, leading to higher emission losses. For the same reason, there are also higher reflection losses since the possibility that the radiation hit a solid surface is higher in low porosity structures.

Considerations

From the numerical study reported before, it turns out that, it is possible to obtain high values of efficiency with a structure presenting at the same time a high volumetric heat transfer coefficient, a high porosity and a variable absorption coefficient that could be adapted to different radiative needs: to contain the emission losses from the inlet zone (low absorption – inlet zone) but also be able of gaining all the power from the incoming radiation source (high absorption– inner zone).

In this regard, further simulations through the continuum approach have been made.

Particularly, in order to demonstrate the considerations reported above, a theoretical simulation case has been introduced with regards to the radiative behavior, acting directly on the setting of the absorption coefficient.

Here, a function that varies along the z-axis has been set as follow:

- $\alpha(z) = 0$ m^{-1} with $(0.0 \leq z < 0.5)$ cm;
- $\alpha(z) = 200$ m^{-1} with $z > 0.5$ cm.

This homogeneous simulation represents a theoretical graded porosity structure, with very high porosity in the front, in correspondence of $\alpha(z) = 0$ m^{-1} with $(0.0 \leq z < 0.5)$, and a higher porosity for the developing structure $\alpha(z) = 200$ m^{-1} with $z > 0.5$ cm.

Furthermore, constant parameters have been set as follow:

- ε = 0.70;
- $h \cdot A_v$ = 3.0 x 10^4 W · m^{-3} · K;
- σ = 0 m^{-1};

The results of this simulation have been compared with another numerical case presenting the same parameters and settings, except for the absorption coefficient that has been considered constant and equal to 200 m^{-1}.

The temperature profiles reported in Fig. 8, show an overall better behavior in the case with variable absorption where the outlet temperature of the fluid is higher. This is due to the reduced radiative losses in case two that allow us to obtain a higher efficiency value.

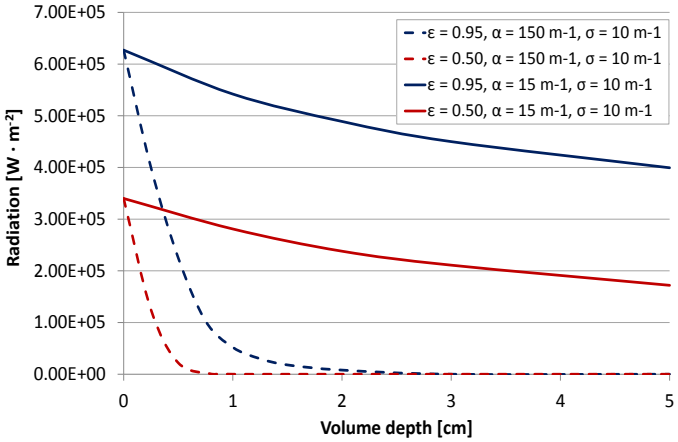

Figure 7 – Radiation vs volume depth for α = (15, 150) m^{-1}, ε = (0.50, 0.95), σ = 10 m^{-1} and $(h \cdot A_v)$ = 30.0 x 10^4 $W \cdot m^{-3} \cdot K$,.

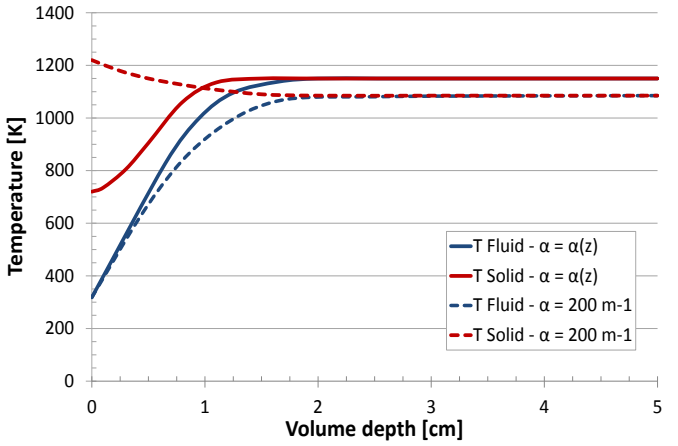

Figure 8 – Temperature profiles vs volume depth obtained through continuum simulation for cases with $\alpha = \alpha(z)$ and α = 200 m^{-1}.

It must be said that the absorption coefficient is strictly related to the porosity of the structure: low absorption can be obtained with high porosity samples and vice versa.

This last numerical exercise, lead to a further consideration regarding the upcoming design procedure: a good compromise will be a structure that presents very thin walls, in order to have a high porosity but also a high cellularity and a graded geometry that presents a higher value of porosity at the inlet zone compared to the rear volume.

Discrete model – simulation results

In this paragraph, the results of the discrete simulation approach will be presented.

The following initial conditions have been set for the discrete simulation:

- G = 6.5 x 10^5 $W \cdot m^{-2}$;
- $\dot{m}$ = 4.8 x 10^{-6} $kg \cdot s^{-1}$;
- $k_{s-a} = \overline{k_{s-a}(T_s)}$ = 22 $W \cdot m^{-1} \cdot K^{-1}$;
- $\hat{\alpha}$ = 0.9;
- T_{f-in} = 318.25 K;
- $P_{f-in} = P_{f-out}$ = 101325 Pa.

In the chart in Fig. 9, temperature profiles of the innovative structure are reported and compared to the ones of the *state-of-the-art* obtained in the same numerical conditions through discrete simulation. The innovative structure shows a better behavior concerning the radiative needs. Thanks to its particular inlet profile characterized by very high porosity and, as a consequence, a very low absorption coefficient, the incoming radiation easily reaches the inner zone. Thus, the front solid area is kept at a relatively low temperature, reducing the losses for re-emission.

Moreover, the equilibrium between the solid and the fluid temperature is reached within 1.5 cm, drastically reducing the required depth of the porous absorber.

For the test sample, the efficiency has been evaluated according to Eq. 13 and compared to the in-house *state-of-the-art* one, using the same numerical approach and the same initial conditions. The calculated efficiencies are:

- $\eta_{i.s.}$ = 0.87;
- η_{s-o-a-} = 0.73.

CONCLUSIONS

In the presented study, a preliminary parametric analysis through continuum simulation has been carried out in order to evaluate the effect of the variation of effective properties and parameters on the performances of a volumetric solar receiver. Here, the porous medium has been represented by the use of a homogeneous volume.

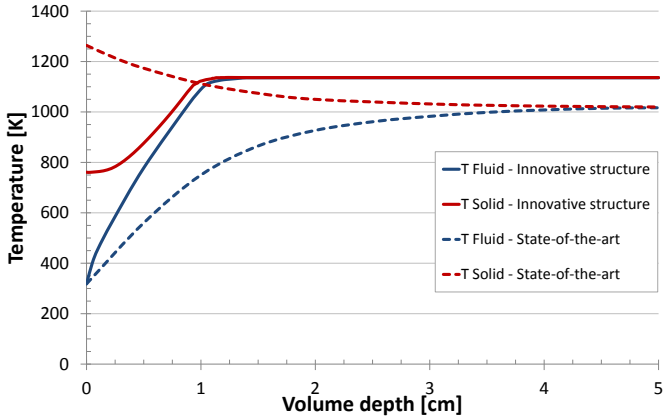

Figure 9 – Temperature profiles vs volume depth obtained through discrete simulation of the innovative structure and the in-house *state-of-the-art*.

This work has led to several conclusions regarding the optimization of porous material structures. In order to have high performance, they must present at the same time high porosity, high thermal exchange surface and a shape that is well adapted to the different radiative needs.

From a design point of view, these remarks translate into a structure presenting very thin walls, a staggered inner geometry and a variable porosity that keeps a higher value in the front in order to allow a better penetration of the radiation, thus reducing reflection and emission losses.

Following these considerations, an innovative absorber structure has been designed to be used as volumetric solar receiver. The same structure has been numerically tested with the use of a discrete numerical model in which the real geometry has been used in the computational domain, showing an improved radiative behavior thanks to its graded porosity and a reduced depth required, showing an increased value of the efficiency.

In the near future, the geometry will be produced by an in-house company in the form of a prototype sample using an austenite nickel-chromium-based alloy for the production. Then, experimental evaluation of the performance will be done using the HLS solar simulator setup in order to validate the previously determined numerical results.

ACKNOWLEDGMENTS

This work was carried out with financial support from the Ministry of Innovation, Science and Research of the State of North Rhine-Westphalia (MIWF NRW), Germany under contract 323-2010-006 (Start-SF).

REFERENCES

1. Romero, M., Buck, R., Pacheco, J.E., 2002. An update on solar central receiver systems, projects, and technologies. Journal of Solar Energy Engineering 124 (2), 98–108.

2. Fricker, H. W., Winkler, C., Silva, M., Chavez, J., 1988. Design and Tests Results of the Wire Receiver Experiment Almeria. Proc. 4th Int. Symp. Solar Thermal Technology, Santa Fe, NM.

3. Buck, R., 1988. Tests and Calculations for a Volumetric Ceramic Receiver, Proc. 4th Int. Symp. Solar Thermal Technology, Santa Fe, NM.

4. Meningault, T., Flamant, G., Rivoire, B.,1991, Advanced High-Temperature Two-Slab Selective Volumetric Receiver. Solar Energy Materials & Solar Cells, (24), 192-203.

5. Hoffschmidt, B., Téllez, F. M., Valverde, A., Fernández, J., Fernández, V., 2003. Performance Evaluation of the 200-kWth HiTRec-II Open Volumetric Air Receiver, Journal of Solar Energy Engineering 125(1), 87-94.

6. Wu, Z., Caliot, C., Flamant, G., Wang, Z., 2011. Coupled radiation and flow modeling in ceramic foam volumetric solar air receivers, Solar Energy 85, 2374-2385.

7. Petrasch, J.; Haussener, S.; Lipinski, W.; Discrete vs. continuum-scale simulation of radiative transfer in semitransparent two-phase media; Journal of Quantitative Spectroscopy and Radiative Transfer, 112(9), 2011.

8. Caliot, C.; Wu, Z.; Flamant, G.; Wang, Z.; Numerical simulation of convective heat transfer between air flow and ceramic foams to optimize volumetric solar air receiver performances; International Journal of Heat and Mass Transfer, 2011.

9. Smirnova, O., Fend, T., Schwarzbözl P., Schöllgen, D., Homogeneous and Inhomogeneous Model for Flow and Heat Transfer in Porous Materials as High Temperature Solar Air Receiver, Proc. of the European COMSOL Conference 2010.

10. A. Kribus, A., Grijnevicha, M., Graya, Y., Caliot, C., 2014. Parametric Study of Volumetric Absorber Performance, Energy Procedia 49, 408-417.

11. Wu, Z., Caliot, C., Flamant, G., Wang, Z., 2011, Numerical simulation of convective heat transfer between air flow and ceramic foams to optimise volumetric solar air receiver performances, International Journal of Heat and Mass Transfer, 54, (7-8), 1527–1537.

12. Capuano R., Comprehensive numerical approach for the design and optimization of solar absorber microstructures, 10th Sollab Doctoral Colloquium on Solar Concentrating Technologies; June 23 – 25, 2014; Odeillo - Font Romeu, France

13. Fiveland, W. A., 1988, Three-dimensional radiative heat-transfer solutions by the discrete-ordinates method, Journal of Thermophysics and Heat Transfer, 2 (4), 309-316..

14. Fend, T., Hoffschmidt, B., Pitz-Paal, R., Reutter, O., Rietbrock, P., 2004, Porous materials as open volumetric solar receivers: experimental determination of thermophysical and heat transfer properties, Energy 29, 822-833.

15. Capuano R., Fend T., Hoffschmidt, B., A comprehensive numerical tool for performance evaluation and design of porous ceramic microstructures in solar thermal application, Gordon Research Conference: Solid State Studies in Ceramics - Jul 20-25, 2014, Mount Holyhoke College, MA, US.

16. Haussener, S., Coray, P., Lipiński, W., Wyss, P., Steinfeld, A., 2009, Tomography-Based Heat and Mass Transfer Characterization of Reticulate Porous Ceramics for High-Temperature Processing, ASME Journal of Heat Transfer 132(2).

17. Hoffschmidt,B.:Vergleichende Bewertung verschiedener Konzepte volumetrischer Strahlungsempfänger, Deutsches Zentrum für Luft- und Raumfahrt e.V., RWTH Dissertation,1996.

18. Pitz-Paal, R., Hoffschmidt, B., Böhmer, M., Becker, M., 1997, Experimental and numerical evaluation of the performance and flow stability of different types of open volumetric absorbers under non-homogeneous irradiation, Solar Energy 60 (3-4), 135-150.

19. Munro, R. G., 1997, Material Properties of a Sintered alpha-SiC, Journal of Physical and Chemical Reference Data, 26, 1195-1203.

20. CapuanoR., Bianco N., Chiu, W. K. S., Cunsolo,S., Naso, V., Oliviero, M., Numerical Analysis of Conjugate Heat Transfer in Foams; COMSOL Conference, 10th – 12th, 2012, Milan, Italy.